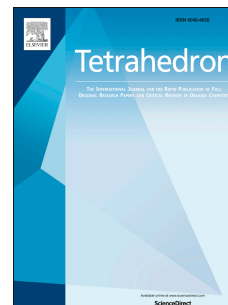# Accepted Manuscript

Bioimprinted lipases in PVA nanofibers as efficient immobilized biocatalysts

Diána Weiser, Péter L. Sóti, Gergely Bánóczi, Viktória Bódai, Bálint Kiss, Ákos Gellért, Zsombor K. Nagy, Béla Koczka, András Szilágyi, György Marosi, László Poppe

Please cite this article as: Weiser D, Sóti PL, Bánóczi G, Bódai V, Kiss B, Gellért E, Nagy ZK, Koczka B, Szilágyi A, Marosi G, Poppe L, Bioimprinted lipases in PVA nanofibers as efficient immobilized biocatalysts, *Tetrahedron* (2016), doi: 10.1016/j.tet.2016.06.027.

This is a PDF file of an unedited manuscript that has been accepted for publication. As a service to our customers we are providing this early version of the manuscript. The manuscript will undergo copyediting, typesetting, and review of the resulting proof before it is published in its final form. Please note that during the production process errors may be discovered which could affect the content, and all legal disclaimers that apply to the journal pertain.

Graphical Abstract

To create your abstract, type over the instructions in the template box below.
Fonts or abstract dimensions should not be changed or altered.

Bioimprinted lipases in PVA nanofibers as efficient immobilized biocatalysts

Leave this area blank for abstract info.

Diána Weiser[a,b,c], Péter L. Sóti[a], Gergely Bánóczi[a], Viktória Bódai[b], Bálint Kiss[d], Ákos Gellért[e], Zsombor K. Nagy[a], Béla Koczka[b], András Szilágyi[c], György Marosi[a], László Poppe[a,d]

[a] Department of Organic Chemistry and Technology, Budapest University of Technology and Economics (BME), Hungary; [b] Fermentia Ltd, Budapest, Hungary; [c] Department of Inorganic and Analytical Chemistry, BME, Hungary; [d] Department of Physical Chemistry and Materials Science, BME, Hungary; [e] Agricultural Institute, Centre of Agricultural Research, Hungarian Academy of Sciences, Martonvásár, Hungary; [f] SynBiocat Ltd, Budapest, Hungary
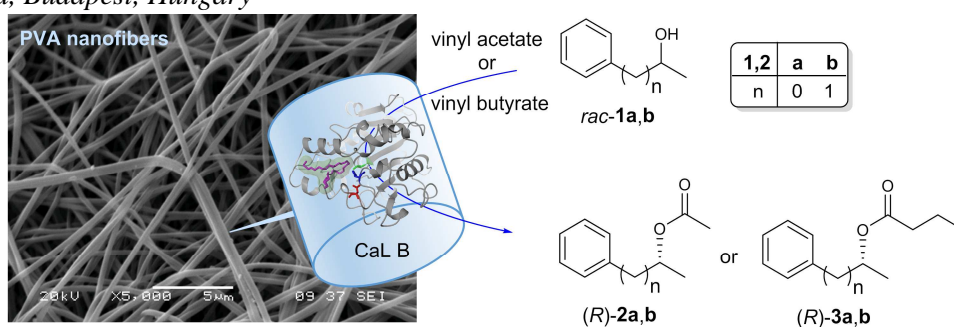
1,2	a	b
n	0	1

Bioimprinted lipases in PVA nanofibers as efficient immobilized biocatalysts

Diána Weiser[a,b,c], Péter L. Sóti[a], Gergely Bánóczi[a], Viktória Bódai[b], Bálint Kiss[d], Ákos Gellért[e], Zsombor K. Nagy[a], Béla Koczka[f], András Szilágyi[d], György Marosi[a], László Poppe[a,c] *

[a] *Department of Organic Chemistry and Technology, Budapest University of Technology and Economics, Műegyetem rkp. 3, H-1111 Budapest, Hungary*

[b] *Fermentia Ltd., Berlini út. 47-49, H-1049, Budapest, Hungary*

[c] *SynBiocat Ltd., Lövőház u 19/1, H-1024 Budapest, Hungary*

[d] *Department of Physical Chemistry and Materials Science, Budapest University of Technology and Economics, Budafoki út 8, H-1111 Budapest, Hungary*

[e] *Agricultural Institute, Centre of Agricultural Research, Hungarian Academy of Sciences, Brunszvik u. 2, H-2462 Martonvásár, Hungary*

[f] *Department of Inorganic and Analytical Chemistry, Budapest University of Technology and Economics, Szt. Gellért tér 4, H-1111 Budapest, Hungary*

ARTICLE INFO

ABSTRACT

Immobilization of lipases from *Pseudomonas fluorescens* (Lipase AK), *Burkholderia (Pseudomonas) cepacia* (Lipase PS) and lipase B from *Pseudozyma (Candida) antarctica* (CaLB) was investigated by entrapment in electrospun poly(vinyl alcohol) (PVA) nanofibers. The activity and selectivity of the lipases entrapped in PVA nanofibers were characterized in kinetic resolution of racemic secondary alcohols using acylation in organic media. Potential bioimprinting effect of eight substrate mimicking additives [polyethylene glycols (PEGs), non-ionic detergents (NIDs) and various organosilanes] was tested with the fiber-entrapped lipases. The nanofibrous lipase biocatalyst entrapped in the presence of the additives were also characterized by rheology, differential scanning calorimetry and scanning electron microscopy. In addition to the known lipase-bioimprinting agents (PEGs, NIDs), phenyl- and octyltriethoxysilane also enhanced substantially the biocatalytic properties of lipases in their electrospun PVA fiber-entrapped forms. The reasons of bioimprinting effect of several additives were rationalized by docking studies in the open and closed form of CaLB.

―――――
* Corresponding author. Tel.: +36-1-463-3299; fax: +36-1-463-3297; e-mail: poppe@mail.bme.hu

1. Introduction

Lipases accept a quite broad range of substrates in mild and selective reactions and therefore widely used in various applications such as industrial biotransformations, immunosensing and biomedical processes.[1] As general requirement for a successful application, these catalysts must be stable and fully functional under process conditions. The process conditions such as temperature, presence of organic (co)solvent, pH-value or pressure quite often differ from the natural environment of enzymes. Enzyme immobilization methods may offer possibilities for the physical stabilization.[2] Immobilized enzymes are advantageous in various commercial applications due to the convenience in handling, the ease of separation of enzymes from the reaction mixture and reuse, the lowered production costs and the possible increase in thermal and pH stability. A carrier or an entrapment matrix for enzyme immobilization should be biocompatible and should provide an inert environment for the enzyme molecules keeping the native conformation of the enzymes and not compromising their biological activity. Although entrapment is a generally applicable and robust enzyme immobilization method, many of the traditionally obtained polymeric matrices provide too tight environment for the enzyme molecules thereby reducing their catalytic activity. In case of immobilized enzymes, biocatalysis is carried out in heterogeneous phases, thus diffusion barrier is among the key factors governing the efficiency of the process. In this respect, permeability and diffusion path length of enzyme carrier or entrapment matrix are critical points.[3,4]

Recent developments in nanotechnology have provided a wealth of diverse nano-scaffolds that could potentially serve as supports for enzyme immobilization.[5] Among the several nano-sized materials, polymer nanofibers are promising carriers or entrapment matrices for enzyme immobilization.[6] Traditional methods for polymer fiber production include melt spinning, dry spinning, wet spinning and gel-state spinning. The electrospinning technology allows the production of long, three-dimensional, ultrafine fibers with diameters in the range of a few nanometers to a few microns and lengths up to kilometers by using an electrostatic field.[7] The unique properties of nanofibers could be utilized, such as extraordinarily high surface area per unit mass, very high porosity, tunable pore size, tunable surface properties, layer thickness, high permeability, low basic weight, ability to retain electrostatic charges and cost effectiveness, among others. Although a number examples exist about enzyme immobilization on the surface of nanofibers,[5] only a few experiments were reported on lipase entrapment within nanofibers. For example, lipase from *Pseudomonas fluorescens* (Lipase AK) was already immobilized in polyurethane (PUR) nanofibers,[8] and lipases from *Candida rugosa*,[9] *Rhizopus oryzae*[10] and *Burkholderia cepacia* (Lipase PS)[11] were encapsulated in simple PVA nanofibers.

In our previous study, it was found that electrospun PVA nanofibers were applicable for entrapment of lipase form *Burkholderia cepacia* (Lipase PS) and lipase B from *Candida antarctica* (CaLB). The Lipase PS and CaLB biocatalysts entrapped in PVA nanofibers were durable biocatalysts retaining significant part of their original biocatalytic activity after 10 recycling (40% with Lipase PS; 80% with CaLB).[12]

One of the most successful strategies for enhancing enzyme activity during immobilization involves tuning the shape of the active site of the enzyme by molecular imprinting with substrates or their analogues.[13–15] The mutual effect of bioimprinting influencing the activity and enantioselectivity of lipases was demonstrated by immobilizations using sol-gel entrapment.[16,17]

The bioimprinting effect could be rationalized on the basis of the generally accepted hypothesis of the interfacial activation mechanism. The active site of many lipases in aqueous solution is covered by a flexible region of the enzyme molecule, often called as lid. Interaction with a hydrophobic phase can cause opening of the lid to make the active site accessible.[18,19] This hypothesis is supported by crystal structures of lipases involving open and closed forms.[20,21] Since interfacial activation can cause a dramatic increase in catalytic activity, it is of profound importance for all applications of lipases, and should always be considered when develop immobilization methods.[1] Although bioimprinting proved to be an efficient tool to modulate the properties of entrapped lipases, this strategy has not been combined with entrapment in electrospun nanofibers yet.

Herein we report efficient bioimprinting of three lipases from *Pseudomonas fluorescens* (Lipase AK), from *Burkholderia (Pseudomonas) cepacia* (Lipase PS) and from *Candida antarctica* (CaLB) entrapped in poly(vinyl alcohol) (PVA) nanofibers. Three types of additives, such as polyethylene glycols, non-ionic detergents and organosilanes, were investigated as bioimprinting molecules for the lipases. Polyethylene glycols and non-ionic detergents were already applied as substrate analogs exhibiting bioimprinting effects in sol-gel systems, but their effect in PVA entrapment has not been investigated yet. In a previous study, the bioimprinting effect of several organosilanes applied as silane precursors to form the sol-gel matrix was considered assuming their substrate analog function.[17] In this study the bioimprinting effect of organosilanes such as phenyltriethoxysilane (PTEOS), octyltriethoxysilane (OTEOS) has been clearly demonstrated.

2. Results and discussion

To test the optimal immobilization conditions, various amounts of Lipase AK were entrapped in electrospun PVA fibers (Table 1 and Figure 1). After selecting 5% lipase loading as optimal during PVA entrapment, three different lipases (Lipase AK, Lipase PS and CaLB) were investigated with rationally selected additives as bioimprinting agents (Tables 2, 3 and 4). Catalytic properties of the formed biocatalysts were tested in kinetic resolution (KR) of racemic 1-phenylethanol (*rac*-**1a**) using vinyl acetate as acylating agent (Scheme 1). Finally, the nanofibrous CaLB biocatalysts formed by entrapment in electrospun PVA nanofibers in presence of the additives causing the most significant activity enhancements were tested in KRs of 1-phenylpropan-2-ol (*rac*-**1b**) using vinyl acetate or vinyl butyrate as acylating agents (Scheme 1, Table 5).
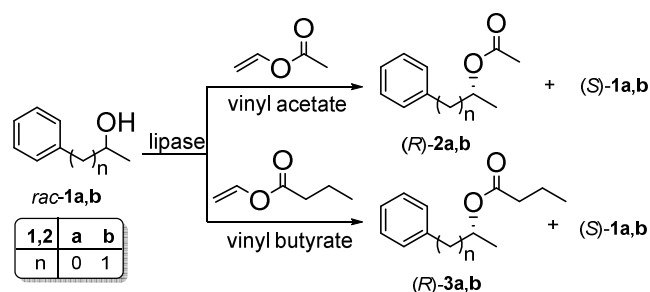
Scheme 1. Kinetic resolution of racemic secondary alcohols (*rac*-**1a,b**) catalyzed by lipase biocatalysts immobilized by entrapment in PVA nanofibers with vinyl acetate or vinyl butyrate as acylating agents.

2.1. Loading of Lipase AK for entrapment in PVA nanofibers

An important goal of enzyme entrapment is to reach an optimal enzyme loading. At optimum, the highest biocatalytic activity can be achieved with the lowest amount of the valuable

enzyme. To optimize enzyme loading in the course of entrapment of Lipase AK in PVA nanofiber, electrospinning was examined at different enzyme/PVA ratios (Table 1 and Figure S1). Catalytic properties of the formed biocatalysts were tested in kinetic resolution of racemic 1-phenylethanol (*rac*-**1a,** Scheme 1 and Table 1) using vinyl acetate as acylating agents.

Although increasing the enzyme loading during PVA nanofiber formation resulted in biocatalysts of increasing activity (*c*) with excellent enantiomeric excess (*ee*$_{(R)\text{-}\mathbf{2a}}$), the standard deviation of these biocatalytic parameters also increased (Table 1). In addition, at high lipase loading nanofiber fabrication become more and more difficult (at enzyme content 33% no nanofiber formation was possible). Moreover, the increase of specific biocatalytic activity (U_B) was not proportional with the lipase loading in nanofibers. The most beneficial activity yield (Y_A = 178%) was observed at 5% lipase loading.

Table 1. Kinetic resolution of 1-phenylethanol (*rac*-**1a)** with Lipase AK in PVA nanofibers of different enzyme loading (time 2 h, reactions in triplicate)

Enzyme content (%)	*c* (%)	*ee*$_{(R)\text{-}\mathbf{2a}}$ (%)	U_B[a] (U g^{-1})	Y_A[b] (%)
100[c]	48.3±0.03	95.2±0.03	33.3	100
5	4.2±0.04	99.4±0.03	2.9	178
10	5.9±0.14	99.4±0.01	4.1	126
15	10.2±0.18	99.6±0.03	7.0	143
20	18.4±0.88	99.6±0.05	12.7	169
25	20.6±1.93	99.5±0.07	14.2	155
33[d]	-	-	-	-

[a] U_B is the effective specific activity of the biocatalyst [U_B= ($n_{rac} \times c$)($t \times m_B$)$^{-1}$], U_E is the effective specific activity of the crude, non-immobilized enzyme [U_E= ($n_{rac} \times c$)($t \times m_E$)$^{-1}$]; [b] Y_A is the activity yield [Y_A= 100×($U_B \times m_B$)/($U_E \times m_E$)]; [c] Crude, non-immobilized Lipase AK; [d] no fiber formation

Scanning electron microscopy (SEM) was used to study the morphology of PVA nanofibers with different lipase loading (it expressed as m/m% compared to the mass of PVA; Figure 1). SEM pictures at 5000× magnification showed significant diversity of fiber uniformity depending on the enzyme content (Figure 1). Without enzyme or at 5% lipase loading, the formed PVA nanofibers were arranged as a well-defined nanostructured tissue with average fiber diameter of 500 nm (Figure 1A). At lipase loading of 10% or above (Figure 1C, D, E, F) nodes and confluences between the polymer fibers appeared and the structure of the nano-tissue was non-uniform. Elementary analysis of nanofibers with higher enzyme loading suggested significant protein aggregation in the non-fibrous area (Figure S6).
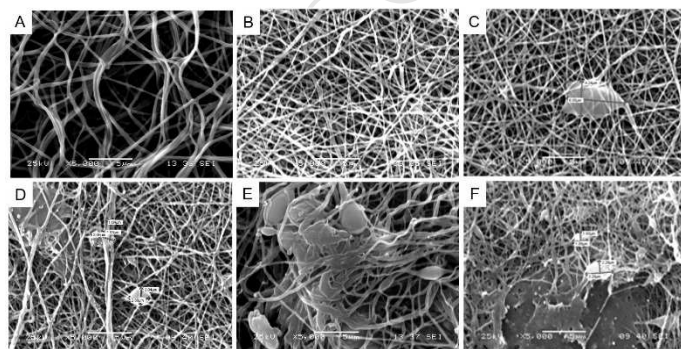

Figure 1. SEM analysis of Lipase AK entrapped in PVA nanofibers at different enzyme content: 0 % (A), 5% (B), 10% (C) 15 % (D), 20% (E) and 25 % (F).

Based on the investigation of catalytic behavior and morphology of the forming fibrous biocatalysts entrapment of

5% Lipase AK was determined as optimal loading in PVA nanofibers to provide a homogenous nanostructured biocatalyst of high activity yield.

2.2. Bioimprinting of lipases in PVA nanofiber

After selecting 5% lipase loading as optimal during PVA entrapment, three different lipases (Lipase AK, Lipase PS and CaLB) were investigated with rationally selected additives as bioimprinting agents. Studies with sol-gel entrapped lipases showed that the "*ligand induced memory*" can also prevail in sol-gel matrices, thus the immobilized lipase can "*remember*" the imprinting effect even after removal of the template molecule.[13] For this reason, selection of proper bioimprinting agents might be crucial to improve the biocatalytic activity and selectivity of the enzymes. Tween 80, Brij 30, PEG, olive oil, lauric acid were studied as potential imprinting agents for lipases in sol-gel matrices.[22] In addition to the fact that the organosilane precursors were able to influence the sol-gel matrix structure, it was assumed that they could act as bioimprinting agents as well.[17] The fact that lipases could accept alkoxysilanes as substrates during oligomerization of dimethlydiethoxysilane (DMDEOS) supported this hypothesis,[23] but in sol-gel systems these influencing factors could not be isolated from each other. Therefore, in this study four different organosilanes (TEOS, PTEOS, OTEOS and DMDEOS) were investigated for the first time as bioimprinting additives – besides four well-known bioimprinting molecules (Brij 30, Tween 80, PEG 400 and PEG 1000) – to enhance the biocatalytic properties of lipases entrapped in PVA nanofibers.

The three different lipases (Lipase AK, Lipase PS and CaLB) entrapped in PVA nanofiber in the presence of the potential bioimprinting agents (PEGs, NIDs and organosilanes) were tested in KR of 1-phenylethanol *rac*-**1a** with vinyl acetate (Tables 2, 3 and 4).

Immobilization of Lipase AK (from *Pseudomonas fluorescens*) in PVA nanofiber in presence of bioimprinting agents resulted in improved activity yield (Y_A) as compared to the entrapment without additive (Table 2). Moreover, the enantiomeric excess values (*ee*$_{(R)\text{-}\mathbf{2}}$) also improved in each case compared to the *ee* values achieved with the native Lipase AK (*ee*$_{(R)\text{-}\mathbf{2a}}$= 99.4%) or Lipase AK in PVA without additive (*ee*$_{(R)\text{-}\mathbf{2a}}$= 95.2%), particularly when Tween 80 [(Y_A= 931%, *ee*$_{(R)\text{-}\mathbf{2a}}$= 99.8%)] or PEG 400 [($Y_A$= 885%, *ee*$_{(R)\text{-}\mathbf{2a}}$= 99.7%)] were applied as bioimprinting additives. Among the organosilanes, PTEOS [(Y_A= 290%, *ee*$_{(R)\text{-}\mathbf{2a}}$ = 99.6 %)] and OTEOS additives [(Y_A= 275%, *ee*$_{(R)\text{-}\mathbf{2a}}$= 99.7%)] as additives enhanced the specific enzyme activity (Table 2).

Table 2. Effect of bioimprinting agents on performance of PVA-entrapped Lipase AK in kinetic resolution of 1-phenylethanol *rac*-**1a** with vinyl acetate (reaction time 2 h)

Additive	*c* (%)	*ee*$_{(R)\text{-}\mathbf{2a}}$ (%)	U_B[a] (U g^{-1})	Y_A[b] (%)
[c]	48.3	95.2	33.3	100
-[d]	4.3	99.4	3.0	178
Brij 30	8.3	99.8	5.7	345
Tween 80	22.5	99.8	15.5	931
PEG 400	21.4	99.7	14.7	885
PEG 1000	3.9	99.6	2.7	160
TEOS	4.5	99.8	3.1	188
PTEOS	7.0	99.6	4.8	290
OTEOS	6.6	99.7	4.6	275
DMDEOS	3.8	99.6	2.6	158

[a] U_B is the effective specific activity of the biocatalyst [$U_B = (n_{rac} \times c)(t \times m_B)^{-1}$], U_E is the effective specific activity of the crude, non-immobilized enzyme [$U_E = (n_{rac} \times c)(t \times m_E)^{-1}$]; [b] Y_A is the activity yield [$Y_A = 100 \times (U_B \times m_B)/(U_E \times m_E)$]; [c] Crude, non-immobilized Lipase AK; [d] Lipase AK entrapped in PVA nanofiber, without additive

The X-ray structure of lipase from *Pseudomonas aeruginosa* (analogous to Lipase AK) complexed with nonaethylene glycol (PDB code: 3CN9)[24] indicated that PEG 400 molecule (consisting 8-9 ethylene oxide monomers) could fit into the active site of the lipase thereby stabilizing the reactive conformation during the immobilization process.

Presence of bioimprinting additives in immobilization of Lipase PS (from *Burkholderia cepacia*) in electrospun PVA nanofibers also improved the specific activity and the enantiomeric excess (Table 3).

Table 3. Effect of bioimprinting agents on performance of PVA-entrapped Lipase PS in kinetic resolution of 1-phenylethanol *rac*-**1a** with vinyl acetate (reaction time 2 h)

Additive	c (%)	$ee_{(R)\text{-}2a}$ (%)	$U_B{}^a$ (U g^{-1})	$Y_A{}^b$ (%)
[c]	41.7	99.1	28.7	100
-[d]	3.6	98.8	2.5	172
Brij 30	13.6	99.5	9.4	654
Tween 80	11.0	99.8	7.6	526
PEG 400	42.2	99.7	29.1	2022
PEG 1000	2.3	98.7	1.6	109
TEOS	3.0	99.1	2.0	142
PTEOS	6.5	99.6	4.5	312
OTEOS	5.1	99.2	3.5	242
DMDEOS	1.9	98.6	1.3	92

[a] U_B is the effective specific activity of the biocatalyst [$U_B = (n_{rac} \times c)(t \times m_B)^{-1}$], U_E is the effective specific activity of the crude, non-immobilized enzyme [$U_E = (n_{rac} \times c)(t \times m_E)^{-1}$]; [b] Y_A is the activity yield [$Y_A = 100 \times (U_B \times m_B)/(U_E \times m_E)$]; [c] Crude, non-immobilized Lipase PS; [b] Lipase PS entrapped in PVA nanofiber, without additive

The PEG 400 additive showed the extremely large enhancement in specific enzyme activity of PVA-entrapped Lipase PS with excellent *ee* (Y_A= 2022%, $ee_{(R)\text{-}2a}$= 99.7 %). This beneficial effect of PEG 400 can be explained also by the X-ray structure of *Pseudomonas cepacia* (PDB code: 5LIP), where a 1,2-bis-octylcarbamoyloxy-ethylester in the active site (comparably long to PEG 400) could maintain the reactive conformation of the enzyme.[25] PTEOS and OTEOS organosilanes were also beneficial for the enzyme activity of entrapped Lipase PS. Notable, that PTEOS could improve not only the activity yield (Y_A= 312%) but also the enantiomeric excess ($ee_{(R)\text{-}2a}$ = 99.6%).

The three-dimensional structure of the lipase B from *Pseudozyma (Candida) antarctica* (CaLB) has been resolved by Uppenberg.[26,27] CaLB contains only a small lid covering the active site.[28] Therefore, it was thought earlier that the typical interfacial activation of lipases[18,19] is not a characteristic feature of this enzyme.[29] However, recent structural investigations revealed the open and closed states of *Ca*LB and the mechanism of interfacial activation.[30] The fact that CaLB is one of the most studied enzyme and this recently discovered interfacial activation mechanism focused our interest to investigate this lipase in the most detail.

Immobilization by electrospinning entrapment within PVA nanofibers enhanced significantly the enzyme activity of entrapped CaLB (Table 4).

Table 4. Effect of bioimprinting agents on performance of PVA-entrapped CaLB in kinetic resolution of 1-phenylethanol *rac*-**1a** with vinyl acetate (reaction time 2 h)

Additive	c (%)	$ee_{(R)\text{-}2a}$ (%)	$U_B{}^a$ (U g^{-1})	$Y_A{}^b$ (%)
[c]	8.3	98.7	5.7	100
-[d]	15.0	99.8	10.4	3605
Brij 30	13.0	99.8	9.0	3124
Tween 80	16.6	99.9	11.4	3983
PEG 400	21.3	99.9	14.7	5118
PEG 1000	14.8	99.5	10.2	3553
TEOS	8.8	98.6	6.1	2118
PTEOS	18.6	99.5	12.8	4460
OTEOS	18.8	99.5	12.9	4499
DMDEOS	12.3	99.7	8.5	2957

[a] U_B is the effective specific activity of the biocatalyst [$U_B = (n_{rac} \times c)(t \times m_B)^{-1}$], U_E is the effective specific activity of the crude, non-immobilized enzyme [$U_E = (n_{rac} \times c)(t \times m_E)^{-1}$]; [b] Y_A is the activity yield [$Y_A = 100 \times (U_B \times m_B)/(U_E \times m_E)$]; [c] Crude, non-immobilized CaLB; [a] CaLB entrapped in PVA nanofiber, without additive

Even the simple PVA nanofiber-entrapped CaLB biocatalysts showed thirty times higher activity than the non-immobilized CaLB powder. Addition of the bioimprinting agents further enhanced the catalytic properties of PVA-entrapped CaLB in each cases. Like with the other two lipases, PEG 400 proved to be an especially efficient additive with CaLB resulting in a biocatalyst with more than fifty times higher specific activity as the native powder with enhanced $ee_{(R)\text{-}2a}$ of the product (99.9 %; compared to 98.7% with the native powder). Among the organosilanes PTEOS and OTEOS additives exhibited significant bioimprinting effects on CaLB, with more than forty-four times enhanced specific activity as the native enzyme affording the product (*R*)-**2** in high $ee_{(R)\text{-}2a}$ (99.5 %).

Next, the study was extended to 1-phenylpropan-2-ol (*rac*-**1b**) as another alcohol and to vinyl butyrate as a second acylating agent. The results found for the series of KRs of 1-phenylethanol *rac*-**1a** using vinyl acetate as acylating agent remained partially valid in this extended study of non-immobilized CaLB, CaLB entrapped in pure PVA, or in PVA doped with Brij 30, PEG 400, PTEOS and OTEOS in KRs of 1-phenylethanol *rac*-**1a** with vinyl butyrate and 1-phenylpropan-2-ol *rac*-**1b** with either vinyl acetate or vinyl butyrate as acylating agents (Table 5). As expected, the overall characteristics of the CaLB biocatalysts changed compared to the KR of *rac*-**1a** with vinyl acetate (Table 4) but the most powerful bioimprinting agents Brij 30 and PEG 400 remained quite effective within all series. The organosilanes PTEOS and OTEOS as additives exhibited much less, almost negligible bioimprinting effects on CaLB when applied in the three additional KRs.

To understand at the molecular level the reasons of the outstanding activity enhancement of Brij 30 and PEG 400 and the moderate activity enhancement of substituted organosilanes with relatively large apolar substituents, such as OTEOS and PTEOS, molecular docking and modelling studies were performed in the active sites of the recently published open and a closed lid structures of CaLB (Figure 2).**Error! Bookmark not defined.** Our goal was to draw conclusions based on the predicted states of Brij 30, PEG 400 and the partially hydrolyzed derivatives of OTEOS, PTEOS,

DMDEOS, and bulkiest product (*R*)-**3b** within the open and a closed lid structures of CaLB. The poses found for Brij 30 and PEG 400 in the closed lid structure of CaLB (Figure 2, panels A and C, respectively) were in good agreement with the X-ray structure of CaLB complexed with a long chain methylpenta(oxyethyl) heptadecanoate substrate analogue (PDB code: 1LBT)[26] thus enforcing our conclusions to rationalize the bioimprinting effect of these two additives.

Table 5. Effect of bioimprinting additives on the catalytic properties of PVA-entrapped CaLB in kinetic resolution of racemic secondary alcohols (*rac*-**1a,b**) using vinyl butyrate or vinyl butyrate as acylating agents

Additive	*c* (%)			*ee* (%)			Y_A[a] (%)		
	(*R*)-**2b**[b]	(*R*)-**3a**[c]	(*R*)-**3b**[d]	(*R*)-**2b**[b]	(*R*)-**3a**[c]	(*R*)-**3b**[c]	(*R*)-**2b**[b]	(*R*)-**3a**[c]	(*R*)-**3b**[c]
[d]	21.0	0.8	7.5	99.2	98.4	97.9	100	100	100
-[e]	5.9	0.5	4.3	98.4	96.5	99.6	280	237	115
Brij 30	27.6	16.0	38.2	99.5	99.9	98.3	1311	8496	6362
PEG 400	29.6	14.0	34.3	99.5	99.7	99.0	1406	7438	9157
PTEOS	3.3	0.3	2.1	98.2	95.7	98.7	158	183	354
OTEOS	2.4	0.5	3.3	96.0	97.4	99.0	116	269	542

[a] Y_A is the activity yield [$Y_A = 100 \times (U_B \times m_B)/(U_E \times m_{E'})$]; [b] reaction time: 2 h, [c] reaction time: 10 h, [d] Crude, non-immobilized CaLB; [e] CaLB entrapped in PVA nanofiber, without additive
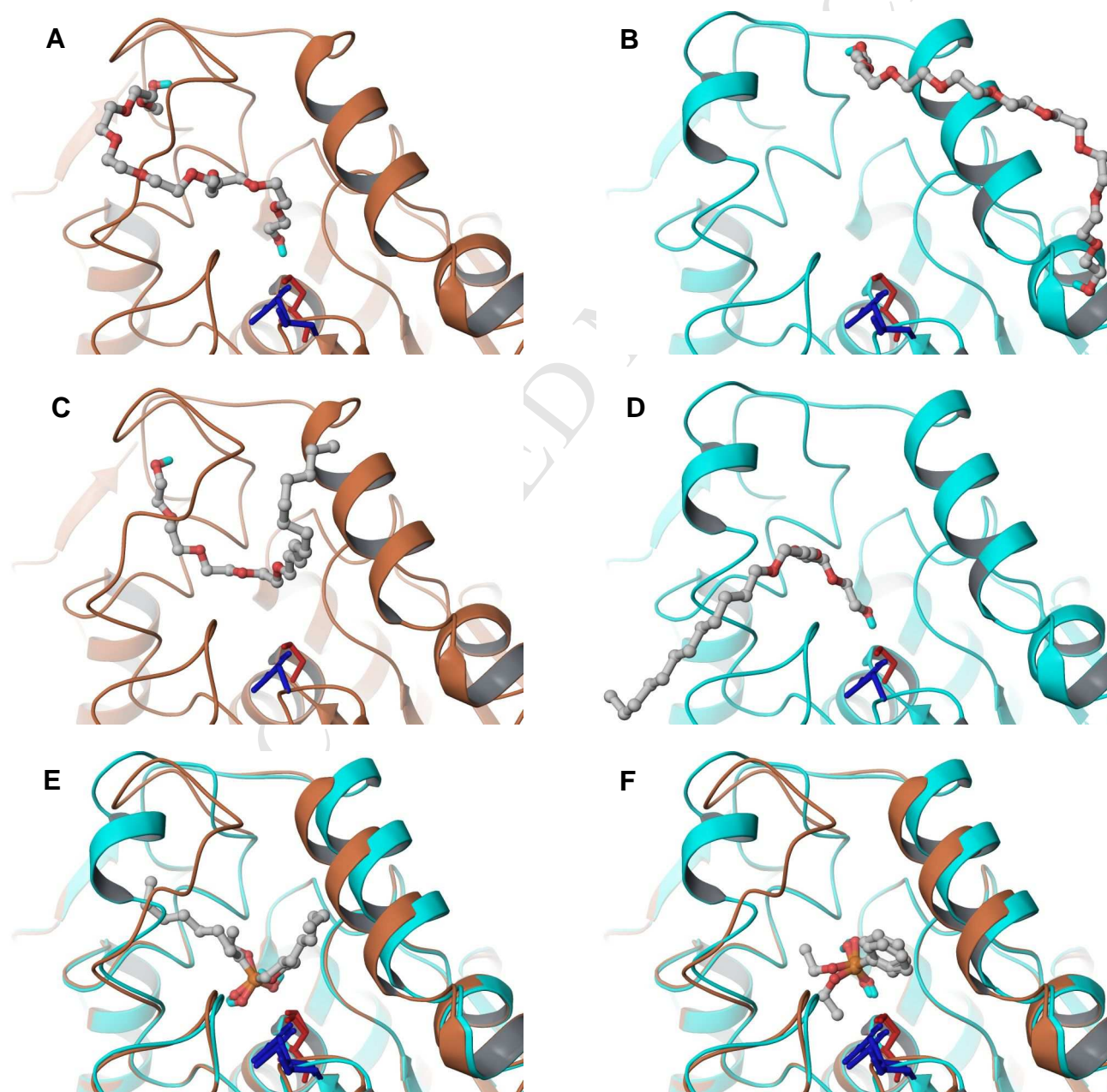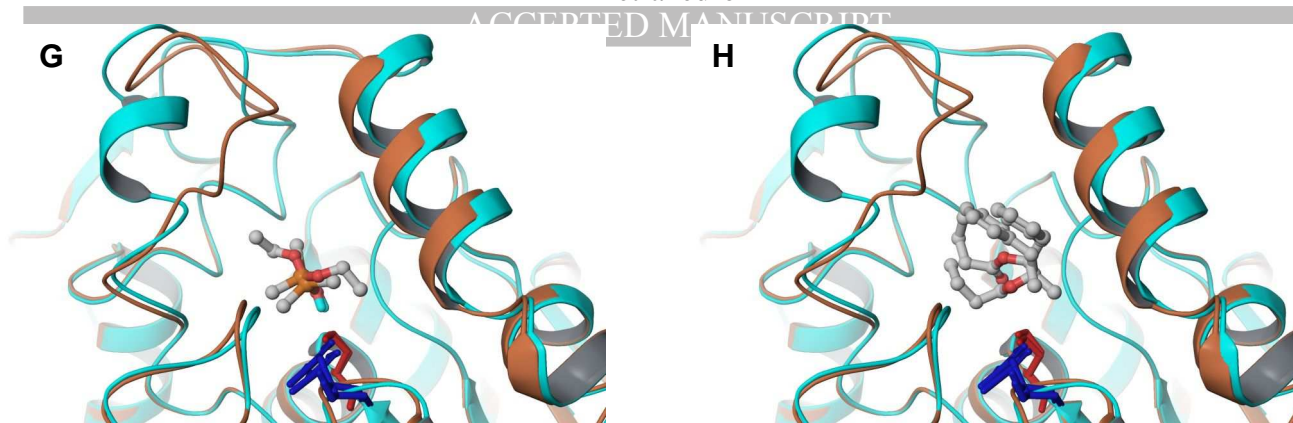
Figure 2. Docking of various additives and the product (*R*)-**3b** into CaLB with open lid conformation (refined model of 5A6V: chain A, in cyan) and CaLB with closed lid conformation (refined model of 5A6V: chain B, in light brown). Panels: (A) Brij 30 in closed CaLB; (B) Brij 30 in open CaLB; (C) PEG 400 in closed CaLB; (D) PEG 400 in open CaLB; (E) overlay of poses of partially hydrolyzed OTEOS in both CaLB forms; (F) overlay of poses of partially hydrolyzed PTEOS in both CaLB forms; (G) overlay of poses of partially hydrolyzed DMDEOS in both CaLB forms; (H) overlay of poses of (*R*)-**3b** in both CaLB forms. Images were created by Maestro.[31]

The docking results revealed that PEG 400 and Brij 30 have distinct arrangements in the case of open CaLB active site (Figure 2, panels A and C, respectively) and in the closed lid conformations (Figure 2, panels B and D, respectively), preferring the binding to closed one with significantly improved affinity values. It could be seen that both additives embrace the mobile lid loop when binding to the closed form. Because of the significantly higher affinity values of the additives to the closed form of CaLB (Table S1), it is probable that during the electrospinning most CaLB molecules adopt such form. This means at the same time protection of the closed reactive form during entrapment and also reserving an enlarged space available for the active site lid after washing out the additive from the active site. The removal of the additives is obvious, otherwise they would act as inhibitors. This double effect – conserving the reactive active site conformation but providing free space to active site lid movements – can significantly improve the catalytic activity during the acylation reactions. Thus the docking study revealed two synergistic effects (reactive conformation stabilization and mobility enhancement of the active lid) resulting in the beneficial bioimprinting effects on CaLB and probably on the other lipases as well.

Based on the experimental results, significant differences were expected between the most effective medium length PEG units-containing additives (Figure 2A-D) and the organosilane compounds (Figure 2E-G). The computed spatial arrangements of the organosilanes were compared to the computed arrangement of the product (*R*)-**3b** (Figure 2H). In all the cases it is clearly visible that the Si atom of the partially hydrolyzed derivatives can occupy a location next to the catalytic serine side chain. Although DMDEOS could be docked also with its Si atom close to the catalytic triad, it seems not large enough to significantly stabilize the active conformation of the active site, while OTEOS and PTEOS share similar sizes and overall arrangements compared to (*R*)-**3b** in both active sites, therefore suggesting overall active site stabilization during immobilization by substrate mimicry. This effect, however, without providing the space for free movements of the active site lid, could cause only much smaller and variable activation.

2.3. Effect of additives on the polymer chain interactions

In case of enzyme entrapment in polymer matrix including nanofibers, the physico-chemical parameters of matrix material may significantly affect the apparent enzyme activity and the final properties of immobilized biocatalyst. Especially interactions between polymer chains can influence the diffusion barriers, which can strongly influence the apparent efficiency of the immobilized biocatalyst. Thus, rheological behavior (dynamic viscosity) of the initial enzyme-polymer-additive mixtures and thermal characteristic [glass transition temperature (T_g) and specific heat capacity (ΔC_p)] of final enzyme-filled nanofibrous materials were also investigated (Table 6).

According to Kramers theory, the biocatalytic activity of enzymes could strongly depend on the viscosity of solvent because viscosity results in friction of proteins in solution leading to decreased motion and inhibiting catalysis in motile enzymes.[32] Thus, viscosity of the medium during entrapment could have an effect on the properties of the immobilized enzyme. In addition, viscosity can significantly influence the fiber formation during electrospinning. The dynamic viscosity of PVA solutions in the presence of the eight different additives were determined by a rheometer. The additive-PVA mixtures were Newtonian fluids with stable viscoelasticity (Figure S2). At the selected 0.06 v/v% concentration, none of the surfactants and organosilanes studied as bioimprinting agents changed significantly the viscosity of the solution compared to the pure PVA solution, except DMDEOS causing a slight increase of the solution's viscosity. Therefore, effects of the additives on the entrapped lipase could not be attributed to a change of the viscosity of the medium.

Table 6. The effect of different additives on the viscosity, glass transition temperature (T_g) and specific heat capacity (ΔC_p) of electrospun PVA nanofibers.

Additive	*Viscosity* (mPas)	T_g (°C)	ΔC_p (J g^{-1}°C^{-1})
-	500.9	71.4	0.30
Brij 30	551.9	66.8	0.24
Tween 80	532.3	67.9	0.29
PEG 400	516.7	45.9	0.08
PEG 1000	525.8	67.7	0.18
TEOS	493.5	71.0	0.28
PTEOS	496.6	70.7	0.29
OTEOS	500.4	70.6	0.30
DMDEOS	575.2	70.8	0.30

Among the additives, only PEG 400 had a significant effect on the T_g of nanofibers (a decrease of T_g 25.5 °C, compared to the PVA fiber without additive). In the case of PEG 400 as additive, the specific heat capacity also decreased significantly, indicating weaker interactions between polymer chains. The higher degree of branching within the entrapment matrix could result in lower diffusion barrier for substrate / product mobility, thereby contributing to the increase of apparent activity of the immobilized lipases.

2.4. Reusability of lipase entrapped in PVA nanofibers

The reusability of CaLB entrapped in PVA nanofibers without and with PEG 400 as additive were investigated in kinetic resolution of *rac*-**1a** in 8 repetitive reaction cycles. The behavior of two biocatalysts were quite similar, the significant part of enzyme activity was conserved after the repeated reaction cycles. The beneficial effect of PEG 400 on the enzyme activity was retained even after 8 runs (Figure 3).

Figure 3. Reusability of CaLB entrapped in PVA nanofibers in kinetic resolution of *rac*-**1a** (2 h at 30 °C; $ee_{(R)\text{-}2a}$ > 95 % in all cases).
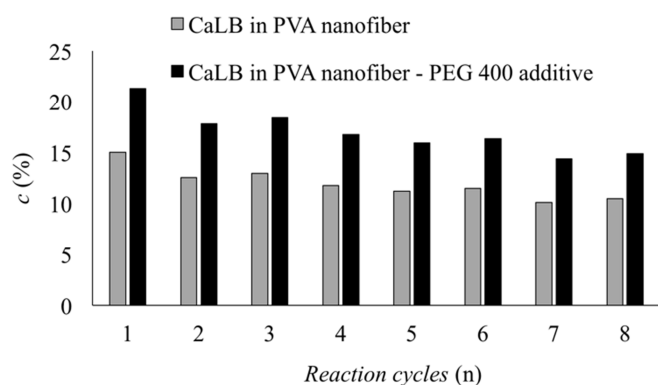
3. Conclusion

Our study demonstrated the bioimprinting effect of substrate mimicking additives (polyethylene glycols, non-ionic detergents and various organosilanes) on lipases entrapped in PVA nanofibers by electrospinning technique. Polyethylene glycol 400 and Tween 80 proved to be the most effective bioimprinting agents, which were able to increase the biocatalytic activity and enantioselectivity of encapsulated lipases. Entrapment of lipases in electrospun nanofibers in presence of organosilanes such as phenyltriethoxysilane and octyltriethoxysilane allowed the demonstration of the real bioimprinting effect of these compounds to enhance the biocatalytic properties of lipases.

This study hypothesized for the first time that minor amounts of well selected additives can cause significant activity enhancement of the entrapped lipases by three factors: i) by stabilizing the active conformation of the lipases; ii) by providing extra room for the mobile active site-covering lids after their removal, thus enhancing the turnover frequency of the reaction; iii) by slackening the polymeric chain structure of the entrapment matrix, thus decreasing mass transfer limitations. We could show that in case of PEG 400 being the most effective additive for lipase immobilization by entrapment in PVA nanofibers, all the three factors play a synergistic role.

4. Experimental section

4.1. Materials and enzymes

(±)-1-Phenylethanol (*rac*-**1a**), (±)-1-phenyl-2-propanol (*rac*-**1b**), vinyl acetate, vinyl butyrate, sodium phosphate mono- and dibasic, hydrochloride acid, sodium fluoride, poly(vinyl-alcohol) (PVA, Mowiol® 18-88), tetraethoxysilane (TEOS), phenyltriethoxysilane (PTEOS), octyltriethoxysilane (OTEOS), dimethyldiethoxysilane (DMDEOS), polyethylene glycol 400 (PEG 400), polyethylene glycol 1000 (PEG 1000), polyethylene glycol dodecyl ether (Brij 30), polyethylene glycol sorbitan monooleate (Tween 80), hexane were purchased from Sigma-Aldrich (Saint Louis, MO, USA), Alfa Aesar Europe (Karlsruhe, Germany) or Merck (Darmstadt, Germany). Solvents (hexane, methyl *tert*-butyl ether (MTBE) were obtained from Merck (Darmstadt, Germany). Amano Lipase AK (lipase from *Pseudomonas fluorescens*) and Amano Lipase PS [lipase from *Burkholderia cepacia* (formerly *Pseudomonas cepacia*)] were obtained from Sigma-Aldrich (Saint Louis MO, USA). CaLB as lyophilized enzyme powder (recombinant *Candida antarctica* lipase B) was obtained from c-LEcta (Leipzig, Germany).

4.2. Entrapment of lipases in PVA nanofibers by electrospinning

For enzyme loading experiments with Lipase AK (Table 1), enzyme solution (100 µL; containing 35.5, 75, 119, 169, 225 and 332 mg mL^{-1} of lipase AK) was prepared in sodium phosphate buffer (0.1 M, pH 7.5) and was added to PVA solution (675 mg; 10 m/m% PVA in distilled water). The Lipase AK containing PVA solution was sonicated for 25 min at 22 °C.

For bioimprinting experiments with lipases (Lipase AK, Lipase PS or CaLB), enzyme solution (100 µL; 35.6 mg mL^{-1} of lipase) was prepared in sodium phosphate buffer (0.1 M, pH 7.5). The enzyme solution and the corresponding additive (5 µL) were added to PVA solution (675 mg; 10 m/m% PVA in distilled water). The PVA solution containing the lipase and the bioimprinting agent was sonicated for 25 min at 22 °C.

For electrospinning the lipase-containing PVA solutions were transferred into a syringe (1 mL) and were fed to the emitter at 0.8–1.00 mL h^{-1} rate using a syringe pump (Aitecs SEP-10S Plus, Vilnius, Lithuania). The distance between the collector and the emitter (with 0.7 mm internal diameter) of the electrospinning equipment was 10 cm. Constant voltage ranging from 20–30 kV was applied to the emitter using a direct current power supplier (NT-35 High Voltage DC Supply MA2000, Nagykanizsa, Hungary). Electrospun fibers were collected on aluminum foil affixed to the collector. Electrospinning experiments were conducted at room temperature (22±2 °C)

4.3. Kinetic resolution of racemic 1-phenylethanol (rac-1a) and racemic 1-phenyl-2-propanol (rac-1b) catalyzed by nanofibrous PVA-lipase biocatalysts

Immobilized or native lipase (50 mg) was added to a solution of the secondary alcohol (*rac*-**1a** or *rac*-**1b**, 50 µL) in hexane/MTBE/vinyl acetate, or hexane/MTBE/vinyl butyrate 6/3/1 (v/v/v) mixture (1 mL) in a screw capped amber glass vial. The resulting mixture was shaken (1000 rpm) at 30 °C for 2 h. Samples (50 µL) taken from the reactions were diluted with ethanol (1 mL), then analyzed by gas chromatography (GC) on an Agilent 4890 equipment using Hydrodex β-6TBDM column (Machery-Nagel, 25 m x 0.25 mm x 0.25 µm, heptakis-(2,3-di-O-methyl-6-O-t-butyldimethylsilyl)-β-cyclodextrin) as described in the Section 1 of the Supplementary material.

Conversion (*c*), enantiomeric excess (*ee*) were determined from GC data (typical progression curves and GC chromatograms can be found in the Supplementary material). Effective specific activity of the biocatalyst (U_B) was determined using the equation $U_B = (n_{rac} \times c)(t \times m_B)^{-1}$ (where n_{rac} [µmol] is the

amount of the racemic substrate, c [-] is the conversion of the substrate, t [min] is the reaction time and m_B [g] is the mass of the biocatalyst). Effective specific activity of the crude non-immobilized enzyme (U_E) was determined using the equation $U_E = (n_{rac} \times c)/(t \times m_E)$ (where n_{rac}, c and t are as defined above and m_E [g] is the mass of the crude non-immobilized enzyme). The activity yield [Y_A (%)] can be calculated from the effective activity of the immobilized biocatalyst ($U_B \times m_B$) compared to the effective activity of the amount of enzyme entrapped in the preparation ($m_{E'}$) as it would be non-immobilized ($U_E \times m_{E'}$); using the equation $Y_A = 100 \times (U_B \times m_B)/(U_E \times m_{E'})$.

4.4. Rheology

The zero-shear viscosity of pure PVA solution, PVA solutions with different enzyme content and PVA solution with different additives were measured at 25 °C using an Anton Paar Physica MCR 301 rheometer with a conical geometry (diameter of 25 mm/1° cone plate).

4.5. Differential scanning calorimetry measurements

The samples were dried in vacuum (1 mbar, 25 °C, 24 h) and stored in desiccator above silica gel before the differential scanning calorimetry (DSC) measurements. Thermal transitions including glass transition of the samples were studied by DSC using a PerkinElmer Diamond DSC equipment. 5 to 15 mg of samples were heated to 150 °C at 10 °C min^{-1} heating rate, kept there for 2 min to erase thermal history and then cooled down to -20 °C with 10 °C min^{-1} cooling rate. After 2 min holding time, the samples were heated again to 150 °C at 10 °C min^{-1} rate to determine the thermal characteristics.

4.6. Reusability of PVA entrapped lipase

Immobilized lipase (50 mg) was added to a solution of the racemic 1-phenylethanol (*rac*-**1a**, 50 µL; 50.6 mg; 0.41 mmol) in hexane/methyl *tert*-butyl ether/vinyl acetate 6/3/1 (v/v) mixture (1 mL) in a screw capped amber glass vial. The resulting mixture was shaken (1000 rpm) at 30 °C for 2 h. Samples (50 µL) for GC analysis taken from the reactions were diluted with ethanol (1 mL). Immobilized lipase was separated from reaction media, then washed with three times with 5 mL hexane/ MTBE 2/1 v/v and dried under vacuum for 1 h (< 25 mbar). Then fresh solution of the racemic 1-phenylethanol (*rac*-**1a**, 50 µL; 50.6 mg; 0.41 mmol) was added to the immobilized lipase in

hexane/MTBE/vinyl acetate 6/3/1 (v/v) mixture (1 mL) in a screw capped amber glass vial. The reaction was repeated as same way described above.

4.7. Molecular modeling methods

X-ray structure of CaLB [PDB ID: 5A6V][30] chain A (with open lid conformation) and chain B (with closed lid conformation) were completed and adjusted using the Protein Preparation Wizard[33] in four steps: (i) hydrogen atoms were added and bond orders were assigned, (ii) artifacts of the protein crystallization procedure and waters were removed, (iii) hydrogen bond network, tautomeric states, and ionization states were determined and optimized, and (iv) a constrained minimization was performed.

A possible set of states of PEG 400, Brij 30, (*R*)-**3b**, and the partially hydrolyzed derivatives of OTEOS, PTEOS, DMDEOS, bound to CaLB with open lid conformation (refined model of 5A6V: chain A) and CaLB with closed lid conformation (refined model of 5A6V: chain B), were obtained by molecular docking using Glide[34] [standard precision with expanded sampling]. The final, lowest energy binding states were selected for each molecule after MM-GBSA rescoring [force field: OPLS3, solvation model: chloroform with an external relative dielectric constant of 2.0], using Prime.[35]

Acknowledgments

Supplementary Material

Supplementary material on elemental analysis by ESD, zero-shear viscosity and DSC curves, representative chiral GC data from KR analyses and calculated apparent binding energy data are attached as separate file.

References and notes

1.   Adlercreutz, P. *Chem. Soc. Rev.* **2013**, *42*, 6406–6436.
2.   Liese, A.; Hilterhaus, L. *Chem. Soc. Rev.* **2013**, *42*, 6236–6249.
3.   Hanefeld, U.; Gardossi, L.; Magner, E. *Chem. Soc. Rev.* **2009**, *38*, 453–468.
4.   Cantone, S.; Ferrario, V.; Corici, L.; Ebert, C.; Fattor, D.; Spizzo, P.; Gardossi, L. *Chem. Soc. Rev.* **2013**, *42*, 6262–6276.
5.   Ansari, S.A.; Husain, Q. *Biotechnol. Adv.* **2012**, *30*, 512–523.
6.   Wu, L.; Yuan, X.; Sheng, J. *J. Membr. Sci.* **2005**, *250*, 167–173.
7.   Arinstein, A.; Zussman, E. *J. Pol. Sci. B: Polym. Phys.* **2011**, *49*, 691–707.
8.   Liu, C.X.; Zhang, S.P.; Su, Z.G.; Wang, P. *Bioresour. Technol.* **2012**, *103*, 266–272.
9.   Sakai, S.; Antoku, K.; Yamaguci, T.; Kawakami, K. *J. Biosci Bioeng.* **2008**, *105*, 687–689.
10.   Wang, Y.; Hsieh, Y.L. *J. Memb. Sci.* **2008**, *309*, 73–81.
11.   Swada, K.; Sakai, S.; Taya M. *J. Biosci. Bioeng.* **2012**, *114*, 204–208.
12.   Sóti, P.; Weiser, D.; Vígh, T.; Nagy, Z.; Poppe, L.;Marosi G.; *Bioproc.Biosyst. Eng.* **2015**, submitted.
13.   Dickey, F.H. *Proc. Natl. Acad. Sci. U.S.A.* **1949**, *35*, 227–229.
14.   Rich, J.O.; Mozhaev, V.; Dordick, J.S.; Clark, D.S.; Khmelnitsky, Y.L. *J. Am. Chem. Soc.* **2002**, *124*, 5254–5255.

15.   Mingarro, I.; Abad, C.; Braco, L. *Proc. Nat. Acad. Sci. U.S.A.* **1995**, *92*, 3308–3312.
16.   Cao, X.; Yang, J.; Shu, L.; Yu, B.; Yan, Y. *Proc. Biochem.* **2009**, *44*, 177–182.
17.   Hellner, G.; Boros, Z.; Tomin, A.; Poppe, L. *Adv. Synth. Catal.* **2011**, *353*, 2481–2491.
18.   Verger, R. *Trends Biotechnol.* **1997**, *15*, 32–38.
19.   Reis, P.; Holmberg, K.; Watzke, H.; Leser, M.E.; Miller, R. *Adv. Colloid Interface Sci.* **2009**, *147–148*, 237–250.
20.   Brady, L.; Brzozowski, A.M.; Derewenda, Z.S.; Dodson, E.; Dodson, G.; Tolley, S.; Turkenburg, J.P.; Christiansen, L.; Hugejensen, B.; Norskov, L.; Thim, L.; Menge, U. *Nature* **1990**, *343*, 767–770.
21.   Schrag, J.D.; Li, Y.; Wu, S.; Cygler, M. *Nature* **1991**, *351*, 761–764.
22.   Reetz, M.T.; Tielmann, P.; Wiesenhöfer, W.; Könen, W.; Zonta, A. *Adv. Synth. Catal.* **2003**, *345*, 717–728.
23.   Nishino, H.; Mori, T.; Okahata, Y. *Chem. Commun.* **2001**, 2684–2685.
24.   Pesaresi, A.; Lamba, D. *Biochimie.* **2010**, *92*, 1787–1792.
25.   Lang, D.A.; Mannesse, M.L.; de Haas, G.H.; Verheij, H.M.; Dijkstra, B.W. *Eur. J. Biochem.* **1998**, *254*, 333–340.
26.   Uppenberg, J.; Ohrner, N.; Norin, M.; Hult, K.; Kleywegt, G.J.; Patkar, S.; Waagen, V.; Anthonsen, T.; Jones, T.A. *Biochemistry.* **1995**, *34*, 16838–16851.

27. Uppenberg, J.; Hansen, M.T.; Patkar, S.; Jones, T.A. *Structure (Oxford, U. K.)* **1994**, *2*, 293–308.

28. Salis, A.; Svensson, I.; Monduzzi, M.; Solinas, V.; Adlercreutz, P. *Biochim. Biophys. Acta* **2003**, *1646*, 145–151.

29. Martinelle, M.; Holmquist, M.; Hult, K. *Biochim. Biophys. Acta* **1995**, *1258*, 272–276.

30. Stauch, B.; Fisher, S.J.; Cianci, M. *J. Lipid. Res.* **2015**, *56*, 2348–2358.

31. Maestro, version 10.6, Schrödinger, LLC, New York, NY, USA, **2016**.

32. Uribe, S.; Sampedro, J.G. *Biol. Proced.* **2003**, *5*, 108−115.

33. (a) Protein Preparation Wizard 2016-1: Epik, Version 2.4; Impact, Version 5.9; (b) Satry, G.M.; Adzhigirey, M.; Day, T.; Annabhimoju, R.; Sherman, W. *J. Comput. Aid. Mol. Des.*, **2013**, *27*, 221-234.

34. (a) Glide, version 7.0, Schrödinger, LLC, New York, NY, USA, **2016**; (b) Friesner, R.A.; Banks, J.L.; Murphy, R.B.; Halgren, T.A.; Klicic, J.J.; Mainz, D.T.; Repasky, M.P.; Knoll, E.H.; Shaw, D.E.; Shelley, M.; Perry, J.K.; Francis, P.; Shenkin, P.S. *J. Med. Chem.*, **2004**, *47*, 1739-1749; (c) Friesner, R.A.; Murphy, R.B.; Repasky, M.P.; Frye, L.L.; Greenwood, J.R.; Halgren, T.A.; Sanschagrin, P.C.; Mainz, D.T. *J. Med. Chem.*, **2006**, *49*, 6177-6196; (d) Halgren, T.A.; Murphy, R.B.; Friesner, R.A.; Beard, H.S.; Frye, L.L.; Pollard, W.T.; Banks, J.L. *J. Med. Chem.*, **2004**, *47*, 1750–1759.

35. Prime, version 4.3, Schrödinger, LLC, New York, NY, USA, **2016**.

BUDAPEST UNIVERSITY OF TECHNOLOGY AND ECONOMICS
Department of Organic Chemistry and Technology

PROF. LÁSZLÓ POPPE

Highlights of the manuscript entitled *"Bioimprinted lipases in PVA nanofibers as efficient immobilized biocatalysts"*

➢ Lipases from different strains entrapped in PVA nanofibers by electrospinning technique were applicable in kinetic resolutions of secondary alcohols.

➢ Additives, such as non-ionic detergents and organosilanes have significant effects on the biocatalytic properties of entrapped lipases.

➢ Polyethylene glycol 400 was the most effective activator of the electrospun lipases due its bioimprinting effect on the enzyme and plasticizer effect on PVA polymer chains.

➢ Octyl- and phenyl-substituted organosilanes were identified as novel bioimprinting agents in course of electrospun lipase immobilization.

Postal address: Tel.: (+36-1) 463 3299
H-1111 Budapest, Gellért tér 4, Hungary   Fax: (+36-1) 463 3297
H-1521 Budapest, PO Box 91, Hungary   E-mail: poppe@mail.bme.hu